

# Identification and Quantitation of Changes in the Platelet Activating Factor Family of Glycerophospholipids over the Course of Neuronal Differentiation by High-Performance Liquid Chromatography Electrospray Ionization Tandem Mass Spectrometry

Shawn N. Whitehead, Weimin Hou, Martin Ethier,<sup>†</sup> Jeffrey C. Smith, André Bourgeois, Rachelle Denis, Steffany A. L. Bennett,\* and Daniel Figeys\*

Neural Regeneration Laboratory and Ottawa Institute of Systems Biology, Department of Biochemistry, Microbiology and Immunology, University of Ottawa, Ottawa, ON, Canada, K1H 8M5

Glycerophospholipids are important structural lipids in membranes with changes associated with progressive neurodegenerative disorders such as Alzheimer disease. Synthesis of the platelet activating factor (PAF) glycerophospholipid subclass is implicated in the control of neuronal differentiation and death. In this article, we combine nanoflow HPLC and mass spectrometry to screen, identify, and quantitate changes in glycerophospholipid subspecies, specifically PAF family members, over the course of neuronal differentiation. Furthermore, precursor ion scans for fragments characteristic of PAF phosphocholine family members and the standard additions of PAF subspecies were combined to perform absolute quantitation of PAF lipids in undifferentiated and differentiated PC12 cells. Surprisingly, a marked asymmetry was detected in the two predominant PAF species (C16:0, C18:0) over the course of differentiation. These results describe a new technique for the sensitive analysis of lipids combining nanoflow HPLC, ESI-MS, and precursor ion scan. Limits of detection of as little as 2 pg of PAF and LPC were obtained, and analysis of the lipidome of as little as 70 000 cells was performed on this system. Furthermore, application to the PC12 model identified a quantifiable difference between PAF molecular species produced over the course of neuronal differentiation.

Glycerophospholipids are important structural lipids in neuronal membranes.<sup>1</sup> Both enzymatic modification by phospholipase A<sub>1</sub>, A<sub>2</sub>, C, and D and nonenzymatic oxidation produces key cellular second messengers including arachidonic acid, eicosanoids, diacylglycerols, and platelet activating factors (PAF) and PAF-

like lipids.<sup>2,3</sup> Enhanced synthesis of bioactive glycerophospholipids during brain development is implicated in control of proliferation of neural precursor cells and differentiation of neuronal and glial lineages.<sup>4</sup> In adult tissue, increased glycerophosphocholine and glycerophosphoethanolamine concentrations in brain and cerebrospinal fluid are associated with a more rapid cognitive decline in Alzheimer disease.<sup>5</sup> Changes in the relative ratio of glycerophospholipid subclasses are also believed to both promote neural cell survival and participate in neuronal death in Parkinson's disease, stroke, and spinal cord injury depending upon which subspecies are generated within the injured microenvironment.<sup>2,4,6</sup> Mechanistic insight, however, has been complicated by the difficulties associated with identifying and quantifying changes in individual molecular species within complex biological samples composed of several thousand lipids.

The PAF subclass of glycerophospholipids is purported to be key mediators of neuronal differentiation and neuronal cell death in vitro and in vivo.<sup>7–15</sup> PAF synthesis occurs through two enzymatic pathways: de novo and remodeling (Figure 1). Canoni-

- (2) Farooqui, A. A.; Ong, W. Y.; Horrocks, L. A. *Pharmacol. Rev.* **2006**, *58*, 591–620.
- (3) Maeba, R.; Yusufu, Y.; Shimasaki, H.; Ueta, N. *Lipids* **2002**, *37*, 893–900.
- (4) Farooqui, A. A.; Horrocks, L. A.; Farooqui, T. *J. Neurosci. Res.* **2007**.
- (5) Sweet, R. A.; Panchalingam, K.; Pettegrew, J. W.; McClure, R. J.; Hamilton, R. L.; Lopez, O. L.; Kaufer, D. I.; DeKosky, S. T.; Klunk, W. E. *Neurobiol. Aging* **2002**, *23*, 547–553.
- (6) Bazan, N. G. *Cell. Mol. Neurobiol.* **2006**, *26*, 901–913.
- (7) Bazan, N. G. *Prog. Brain Res.* **1998**, *118*, 281–291.
- (8) Bate, C.; Salmons, M.; Williams, A. *Neuroreport* **2004**, *15*, 509–513.
- (9) Bellizzi, M. J.; Lu, S. M.; Masliah, E.; Gelbard, H. A. *J. Clin. Invest.* **2005**, *115*, 3185–3192.
- (10) Xu, Y.; Zhang, B.; Hua, Z.; Johns, R. A.; Bredt, D. S.; Tao, Y. X. *Exp. Neurol.* **2004**, *189*, 16–24.
- (11) Korneci, E.; Ehrlich, Y. H. *Science* **1988**, *240*, 1792–1794.
- (12) Francescangeli, E.; Domanska-Janik, K.; Goracci, G. *J. Lipid Mediat. Cell Signal* **1996**, *14*, 89–98.
- (13) Francescangeli, E.; Freysz, L.; Goracci, G. *Adv. Exp. Med. Biol.* **1996**, *416*, 21–27.
- (14) Francescangeli, E.; Grassi, S.; Pettorossi, V. E.; Goracci, G. *Neurochem. Res.* **2002**, *27*, 1465–1471.
- (15) Francescangeli, E.; Lang, D.; Dreyfus, H.; Boila, A.; Freysz, L.; Goracci, G. *Neurochem. Res.* **1997**, *22*, 1299–1307.

\* To whom correspondence should be addressed. Fax: (613) 562-5452. E-mail: sbennet@uottawa.ca. Tel: (613) 562-5800 x8372. E-mail: dfigeys@uottawa.ca. Tel: (613) 562-5800 x8674.

<sup>†</sup> Current address: CIPO, 815A, 50 rue Victoria, Gatineau, Québec, K1A 0C9.

(1) Farooqui, A. A.; Horrocks, L. A.; Farooqui, T. *Chem. Phys. Lipids* **2000**, *106*, 1–29.

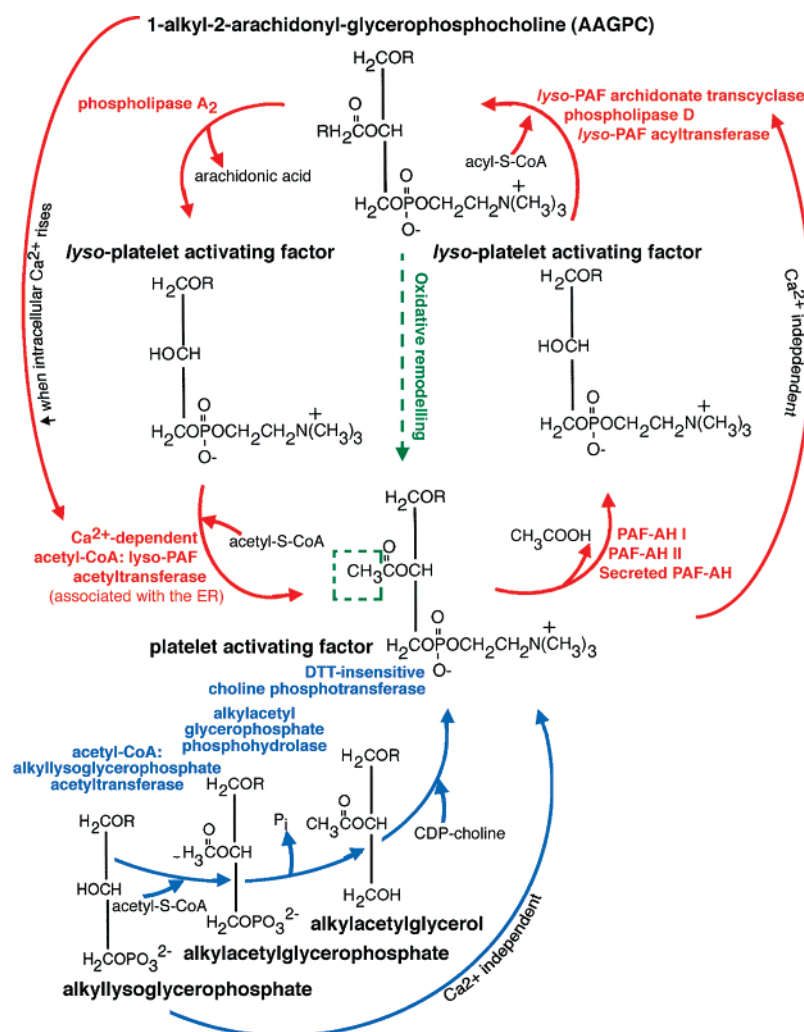


**Figure 1.** Enzymatic and nonenzymatic generation of PAF family members. PAF species are synthesized through the PAF remodeling pathway (red), de novo synthesis (blue), or direct oxidation of membrane lipids (green, enzyme-independent). Predominant molecular species generated by enzymatic synthesis in brain are the C16:0 and C18:0 PAF family members. Oxidation generates PAF-like family members with longer chain fatty acids (up to 8 carbons) at the *sn*-2 position (hatched green box).

cal PAF lipids are defined by alkyl ether linkage at the *sn*-1 position, a short-chain acyl group at the *sn*-2 position, and a phosphocholine, phosphoethanolamine, or phosphatidic acid at the *sn*-3 position; however, 1-acyl-2-acetyl-*sn*-glycero-3-phosphocholine species are also produced at significant levels in brain.<sup>16–19</sup> Moreover, PAF-like lipids with 4–8 carbon side chains at the *sn*-2 position can be generated by nonenzymatic oxidation of *sn*-2 acyl fatty acids chains in structural membrane glycerophospholipids.<sup>20</sup>

It is not known whether specific PAF subspecies are preferentially generated over the course of neuronal differentiation or neurodegenerative disease. Therefore, the importance attributed to PAF synthesis in brain over the course of neurodevelopment and following brain injury highlights the need for a rapid, efficient means of identifying and quantifying changes in subspecies at the

molecular level. Traditionally, PAF detection methodologies have employed two main technologies. Fractionation of lipid extracts by thin-layer chromatography (TLC) isolated from cells labeled with [<sup>3</sup>H]-acetate in the presence of stimuli known to induce PAF synthesis followed by high-performance liquid chromatography (HPLC) and bioassay for PAF-like activities has provided conclusive evidence that neurons, glia, and vascular endothelial cells synthesize PAF lipids.<sup>21–23</sup> Disadvantages of this methodology include the low analytical resolution afforded by TLC,<sup>24</sup> the necessity to prelabel samples in the presence of agonist, and the inability to identify the alkyl and acyl chain compositions. Alternatively, mass spectrometry (MS) combined with capillary or gas chromatography and negative-ion chemical ionization can detect specific glycerophospholipid species in biological samples includ-

(16) Tokumura, A.; Takauchi, K.; Asai, T.; Kamiyasu, K.; Ogawa, T.; Tsukatani, H. *J. Lipid Res.* **1989**, *30*, 219–224.  
 (17) Balestrieri, M. L.; Lee, T. *FEBS Lett.* **2000**, *479*, 63–66.  
 (18) Yue, T. L.; Feuerstein, G. *Crit. Rev. Neurobiol.* **1994**, *8*, 11–24.  
 (19) Farooqui, A. A.; Horrocks, L. A. *Neuroscientist* **2006**, *12*, 245–260.  
 (20) Marathe, G. K.; Harrison, K. A.; Murphy, R. C.; Prescott, S. M.; Zimmerman, G. A.; McIntyre, T. M. *Free Radical Biol. Med.* **2000**, *28*, 1762–1770.

(21) Yue, T. L.; Lysko, P. G.; Feuerstein, G. *J. Neurochem.* **1990**, *54*, 1809–1811.  
 (22) Balestrieri, M. L.; Servillo, L.; Lee, T. *J. Biol. Chem.* **1997**, *272*, 17431–17437.  
 (23) Hanahan, D. J.; Weintraub, S. T. *Methods Biochem. Anal.* **1985**, *31*, 195–219.  
 (24) Peterson, B. L.; Cummings, B. S. *Biomed. Chromatogr.* **2006**, *20*, 227–243.

ing cerebral spinal fluid and has been used to elucidate the predominant 1-alkyl and 1-acyl PAF subclasses as well as oxidized PAF-like lipids produced by neural cells and cerebral endothelia.<sup>16,25–29</sup> Identification, however, depends upon labor-intensive derivatization of target standards prior to analysis and, as such, is not easily amenable to lipid “discovery”. More recently, matrix-assisted laser desorption/ionization time-of-flight (MALDI-TOF) mass spectrometry and electrospray ionization mass spectrometry (ESI-MS) has enabled direct detection and identification of lipid species at the molecular level. MALDI-TOF has identified C14:0 PAF in tears;<sup>30</sup> however, use of this technology is still considered better suited to analysis of high molecular weight protein targets not low molecular weight lipids.<sup>31</sup> The polarity of PAF species requires special matrixes and analytes whose ions are likely also detected in the spectra<sup>32</sup> such that the presence of multiple PAF glycerophosphocholines in a complex sample may mask detection of less abundant subspecies.

To date, LC-ESI-MS has proven the most successful in simultaneous detection of multiple glycerophospholipid subspecies at the molecular level. Application of two-dimensional (2D) maps of elution time and mass provides a useful means of profiling subclasses within complex samples.<sup>33</sup> New tandem mass spectrometry (MS/MS) advances in combination with multiple linear regression modeling has significantly enhanced the capacity to subsequently resolve and quantify molecular subspecies.<sup>34</sup> However, these techniques have yet to be applied to a comparison of lipid species in lipid-enriched neural samples extracted over the course of differentiation or disease. Here, we describe a method to rapidly screen, identify, and quantify changes in glycerophospholipid family members that can be used to compare multiple bioactive subspecies generated over the course of neuronal differentiation. In our approach, nanoflow rate HPLC is combined with positive ion mode ESI-MS to generate 2D profiles of the glycerophospholipid contents of undifferentiated and differentiated PC12 cells. The utilization of precursor ion scans for fragments characteristic of PAF family members and the standard additions of PAF subspecies allow for the absolute quantitation of PAF molecules during cell differentiation. We show, for the first time, that the combination of nanoflow rate HPLC with different MS techniques allows the rapid analysis of lipid extract and the specific quantitation of PAF family members from as little as 70 000 PC12 cells. Furthermore, this study represents the first attempt at the

quantitative study of the changes in the lipidome in a cellular model of neuronal differentiation.

## EXPERIMENTAL SECTION

**Materials.** 1-*O*-Hexadecyl-2-acetyl-*sn*-glycero-3-phosphocholine (C16:0 PAF), 1-*O*-hexadecyl-2-hydroxy-*sn*-glycero-3-phosphocholine (C16:0 *lyso*-PAF), 1-*O*-octadecyl-2-acetyl-*sn*-glycero-3-phosphocholine (C18:0 PAF), and 1-*O*-octadecyl-2-hydroxy-*sn*-glycero-3-phosphocholine (C18:0 *lyso*-PAF) were purchased from Biomol Research Laboratories (Plymouth Meeting, PA). C13:0 lysophosphatidylcholine (C13:0 LPC) was purchased from Avanti Polar Lipids (Alabaster, AL). Stock chemicals were purchased from J.T. Baker (Phillipsburg, NJ) with the exception of bovine serum albumin (BSA) from Sigma (St. Louis, MO).

**Cell Culture.** Rat pheochromocytoma PC12 cells originally obtained from the American Type Tissue Collection were cultured in RPMI containing 10% horse serum and 5% newborn calf serum (complete media) at 37 °C in a 5% CO<sub>2</sub>/95% air atmosphere. PC12 cells were differentiated to a neuronal phenotype by seeding at a density of  $5 \times 10^4$  cells/dish on 10-cm-diameter tissue culture plates coated with 2 μg/mL rat tail collagen (Roche, Mississauga, ON, Canada). Twenty-four hours after plating, cells were cultured in differentiation media (RPMI containing 0.5% heat-inactivated horse serum and 50 ng/mL 7S nerve growth factor (NGF, Sigma)). Cells were fed every second day for 7 days. Untreated controls were seeded at a density of  $1 \times 10^5$  cells/dish and lipids extracted 72 h after plating. Plating controls seeded and cultured at the same time were counted immediately prior to lipid extraction to establish final cell number (PC12 cells  $2.34 \times 10^6$ , NGF-differentiated PC12 cells  $1.79 \times 10^7$ ). All culture reagents were obtained from Invitrogen (Burlington, ON, Canada) except where indicated.

**Glycerophospholipid Extraction.** Glycerophospholipids were extracted according to a modified Bligh/Dyer procedure<sup>35</sup> we have previously published.<sup>36</sup> Briefly, medium was removed from each plate and cells were washed extensively with 10 mM phosphate-buffered saline. Cultures of undifferentiated PC12 and NGF-differentiated PC12 cells were placed on ice, and 1 mL of ice-cold methanol acidified with 2% acetic acid was added to each plate. Cells were then scraped and collected in acidified methanol. Four plates per condition were harvested and pooled. Lipids were extracted using a volumetric ratio of 0.95 of chloroform and 0.8 of 0.1 M sodium acetate (aq) per volume of MeOH in acid-washed borosilicate glass tubes (Fisher, Ottawa, ON, Canada). Phospholipids were collected from the organic phase after layer separation by centrifugation. The aqueous phase was then back-extracted three times in the organic phase of a wash solution prepared by combining RPMI+ 0.025% BSA, methanol, chloroform, and sodium acetate in the volumetric ratio of 1:2.5:3.75:1. The organic fractions were combined, evaporated under a stream of nitrogen gas, and dissolved in 300 μL of EtOH. To assess recovery, cell extracts in acidified methanol were spiked with 100 ng of C16:0 PAF or C16:0 *lyso*-PAF. Recovery was estimated at 94–96%.

**LC-ESI-MS/MS.** Eight microliters of lipid extract was analyzed for each LC–MS run. To account for the differences in cell number between PC12 and NGF-differentiated PC12 cultures, extracts from the differentiated cultures were diluted prior to

(25) Callea, L.; Arese, M.; Orlandini, A.; Bargnani, C.; Priori, A.; Bussolino, F. *J. Neuroimmunol.* **1999**, *94*, 212–221.

(26) Turk, J.; Bohrer, A.; Stump, W. T.; Ramanadham, S.; Mangino, M. J. *J. Chromatogr. Biomed. Appl.* **1992**, *575*, 183–196.

(27) Silvestro, L.; Da Col, R.; Scappaticci, E.; Libertucci, D.; Biancone, L.; Camussi, G. *J. Chromatogr.* **1993**, *647*, 261–269.

(28) Kita, Y.; Takahashi, T.; Uozumi, N.; Shimizu, T. *Anal. Biochem.* **2005**, *342*, 134–143.

(29) Tokumura, A.; Tanaka, T.; Yotsumoto, T.; Tsukatani, H. *J. Lipid Mediat.* **1992**, *5*, 127–130.

(30) Ham, B. M.; Cole, R. B.; Jacob, J. T. *Invest. Ophthalmol. Vision Sci.* **2006**, *47*, 3330–3338.

(31) Schiller, J.; Suss, R.; Arnhold, J.; Fuchs, B.; Lessig, J.; Muller, M.; Petkovic, M.; Spalteholz, H.; Zschornig, O.; Arnold, K. *Prog. Lipid Res.* **2004**, *43*, 449–488.

(32) Schiller, J.; Suss, R.; Fuchs, B.; Muller, M.; Zschornig, O.; Arnold, K. *Front. Biosci.* **2007**, *12*, 2568–2579.

(33) Taguchi, R.; Hayakawa, J.; Takeuchi, Y.; Ishida, M. *J. Mass Spectrom.* **2000**, *35*, 953–966.

(34) Callender, H. L.; Forrester, J. S.; Ivanova, P.; Preininger, A.; Milne, S.; Brown, H. A. *Anal. Chem.* **2007**, *79*, 263–272.

(35) Bligh, E. C.; Dyer, W. J. *Can. J. Biochem.* **1959**, *37*, 911–917.

(36) Bonin, F.; Ryan, S. D.; Migahed, L.; Mo, F.; Lallier, J.; Franks, D. J.; Arai, H.; Bennett, S. A. *J. Biol. Chem.* **2004**, *279*, 52425–52436.

**Table 1. Elution Time and Parent Ion Masses of Candidate PAF Species Detected in NGF-Differentiated PC12 Cells in 2D Spectra of the  $m/z$  184.0 Precursor Ion Scans**

parent ion mass ( $\pm 0.13$ ) <sup>a</sup> ( $m/z$ )	LC elution time ( $\pm 0.4$ ) <sup>a</sup> (min)	candidate PAF species <sup>b</sup>	change in relative abundance following differentiation (per 10 <sup>6</sup> /cells) <sup>c</sup>
482.5	7.98, 8.38, 10.26	<b>C16:0 lyso-PAF, C12:0-acyl-PAF, C15:0-LPC, 14:0<sup>d</sup>, 15:0<sup>e</sup></b>	increase
496.3	9.10	<b>C14:0-PAF</b>	increase
	9.60	<b>C16:0 LPC</b>	no change (endogenous standard)
508.6	8.58, 8.86, 10.88	<b>C17:1-LPC, C18:1-lyso-PAF, 16:1<sup>d</sup>, 17:1<sup>e</sup></b>	increase
510.5	11.08, 14.23	<b>C18:0-lyso-PAF, C17:0-LPC, C14:0-acyl-PAF, 16:0<sup>d</sup>, 17:0<sup>e</sup></b>	increase
524.6	12.19, 13.02	<b>C16:0-PAF, C18:0-LPC, 17:0<sup>d</sup>, 18:0<sup>e</sup></b>	increase
538.4	9.60	<b>C16-acyl-PAF, C19:0-LPC, 18:0<sup>d</sup>, 19:0<sup>e</sup></b>	increase (but eluting at different time after differentiation suggesting a change in species)
546.5	8.36, 9.12	<b>C20:3-LPC, C18:3-PAF, 19:3<sup>d</sup>, 20:3<sup>e</sup></b>	only present after differentiation
548.7	10.55, 11.08	<b>C18:2-PAF, C20:2-LPC, 19:2<sup>d</sup>, 20:2<sup>e</sup></b>	decrease (but increase in the number of species)
550.5	12.88, 13.58	<b>C18:1-PAF, C20:1-LPC, 19:1<sup>d</sup>, 20:1<sup>e</sup></b>	increase (in abundance and number of species)
552.4	-	<b>C18:0-PAF, 20:0-LPC</b>	not detected
574.5	12.18	<b>C20:3-PAF, 21:3<sup>d</sup>, 22:3<sup>e</sup></b>	only present after differentiation
578.7	17.83, 18.95	<b>C20:1-PAF, 21:1<sup>d</sup>, 22:1<sup>e</sup></b>	only present after differentiation
580.7	26.56	<b>C20:0-PAF, C22:0-LPC, 21:0<sup>d</sup>, 22:0<sup>e</sup></b>	only present after differentiation
596.3	9.88	<b>C22:6-PAF, 23:6<sup>d</sup>, 24:6<sup>e</sup></b>	only present after differentiation

<sup>a</sup> Variations between  $m/z$  and retention time between runs were established for 10 glycerophospholipid species over 6 different analyses in both PC12 and NGF-differentiated PC12 cells in 120 different spectra. <sup>b</sup> While our 2D plots indicate changes in multiple glycerophosphocholines over the course of differentiation, here we focus only on PAF species. Identification is predicted based on the theoretical monoisotopic mass values. For PAF species, CX:Y refers to the number of carbon atoms and double bonds in the *sn*-1 chain with a predicted acetyl (PAF) or hydroxyl (*lyso*-PAF) group at the *sn*-2 position. We include non-PAF lipids only where mass is insufficient to distinguish between biologically relevant PAF and other glycerophospholipids. In the case of non-PAF family members, glycerophospholipids are designated as CX:Y, where X represents the total number of predicated carbons at both the *sn*-1 and the *sn*-2 positions and Y the total number of double bonds at both positions. Possible major species are further characterized in footnotes *d* and *e*. <sup>c</sup> Change in relative abundance refers to a change in the sum total corrected intensity of all species at a single  $m/z$  ratio and elution time after differentiation. <sup>d</sup> Diacyl. <sup>e</sup> Alkyl acyl.

analysis. Before being introduced into the LC-MS system, 5  $\mu$ L of a standard solution containing known amounts of C16:0, C18:0 PAF and C16:0, C18:0 *lyso*-PAF were spiked into the sample, and the final volume was brought to 40  $\mu$ L by adding 27  $\mu$ L of H<sub>2</sub>O with 0.1% formic acid. Five standard solutions containing 200, 400, 600, 800, and 1000 pg each of C16:0, C18:0 PAF and C16:0, C18:0 *lyso*-PAF were used in the experiment. At each standard addition concentration, samples were analyzed in triplicate.

A microflow 1100 HPLC system (Agilent, Palo Alto, CA) was used to introduce the analytes into a 2000 Q TRAP mass spectrometer. The solvents used were water and acetonitrile each with 0.1% formic acid (J.T. Baker). Samples were loaded successively onto an Agilent 96-well sampling plate, which was then covered with a preslit well cap and thermostated at 4 °C. An Agilent 1100 autosampler was employed to introduce the analytes onto a 200  $\mu$ m  $\times$  50 mm precolumn packed with 5- $\mu$ m YMC ODS-A C18 beads (Waters, Milford, MA) at a flow rate of 10  $\mu$ L/min. Following the completion of loading 40  $\mu$ L of analyte, the HPLC flow was split and the analyte was eluted through a 75  $\mu$ m  $\times$  50 mm Picotip emitter (New Objective, Woburn, MA), which was interfaced with the mass spectrometer via electrospray ionization, at  $\sim$ 200 nL/min. The emitter was packed with the same beads as those of the precolumn. A linear gradient was used to separate the glycerophospholipid species. The gradient of the HPLC increased from 5 to 60% acetonitrile in 1.5 min, from 60 to 80% acetonitrile over the next 35 min, and from 80 to 95% acetonitrile over the next 4 min. Most of the lipid species were eluted from the columns between 60 and 80% acetonitrile. The

column was then washed with 95% acetonitrile for  $\sim$ 40 min, following which it was regenerated at 95% H<sub>2</sub>O for 15 min.

Data were collected on a 2000 Q-TRAP mass spectrometer operated with Analyst 1.4.1 (Applied Biosystems/MDS Sciex, Concord, ON, Canada). In the detection process, total lipid extract were analyzed by enhanced MS scan. The glycerophosphocholine species were further analyzed in positive ion mode using precursor ion scan for an MS/MS fragment with a mass to charge ratio ( $m/z$ ) of 184.0, a diagnostic fragment of phosphocholine.<sup>37</sup> The resolution for both Q1 and Q3 were set at low to maximize the sensitivity for ion detection. Capillary voltage was 3.5 kV. Nitrogen served as the collision gas, and the collision energy was 40 eV.

**Data Analysis.** Changes in glycerophospholipid profiles over the course of PC12 differentiation were assessed initially by analysis of the elution pattern of total glycerophospholipids and phosphocholine-containing species in 2D maps graphing mass to charge ratio against elution time with relative abundance color coded. Extracted ion chromatograph (XIC)-generated peak areas of LC-MS/MS data were measured using Analyst 1.4.1 (Applied Biosystems/MDS Sciex). Peak areas of C16:0, C18:0 PAF and C16:0, C18:0 *lyso*-PAF at different standard addition points were normalized with respect to that of an internal standard added to each sample C13:0 lysophosphatidylcholine (C13:0 LPC), a lipid that is not naturally occurring in mammalian cells,<sup>38</sup> or an

(37) Brugger, B.; Erben, G.; Sandhoff, R.; Wieland, F. T.; Lehmann, W. D. *Proc. Natl. Acad. Sci. U.S.A.* **1997**, *94*, 2339–2344.

(38) Drobnik, W.; Liebisch, G.; Audebert, F. X.; Frohlich, D.; Gluck, T.; Vogel, P.; Rothe, G.; Schmitz, G. *J. Lipid Res.* **2003**, *44*, 754–761.

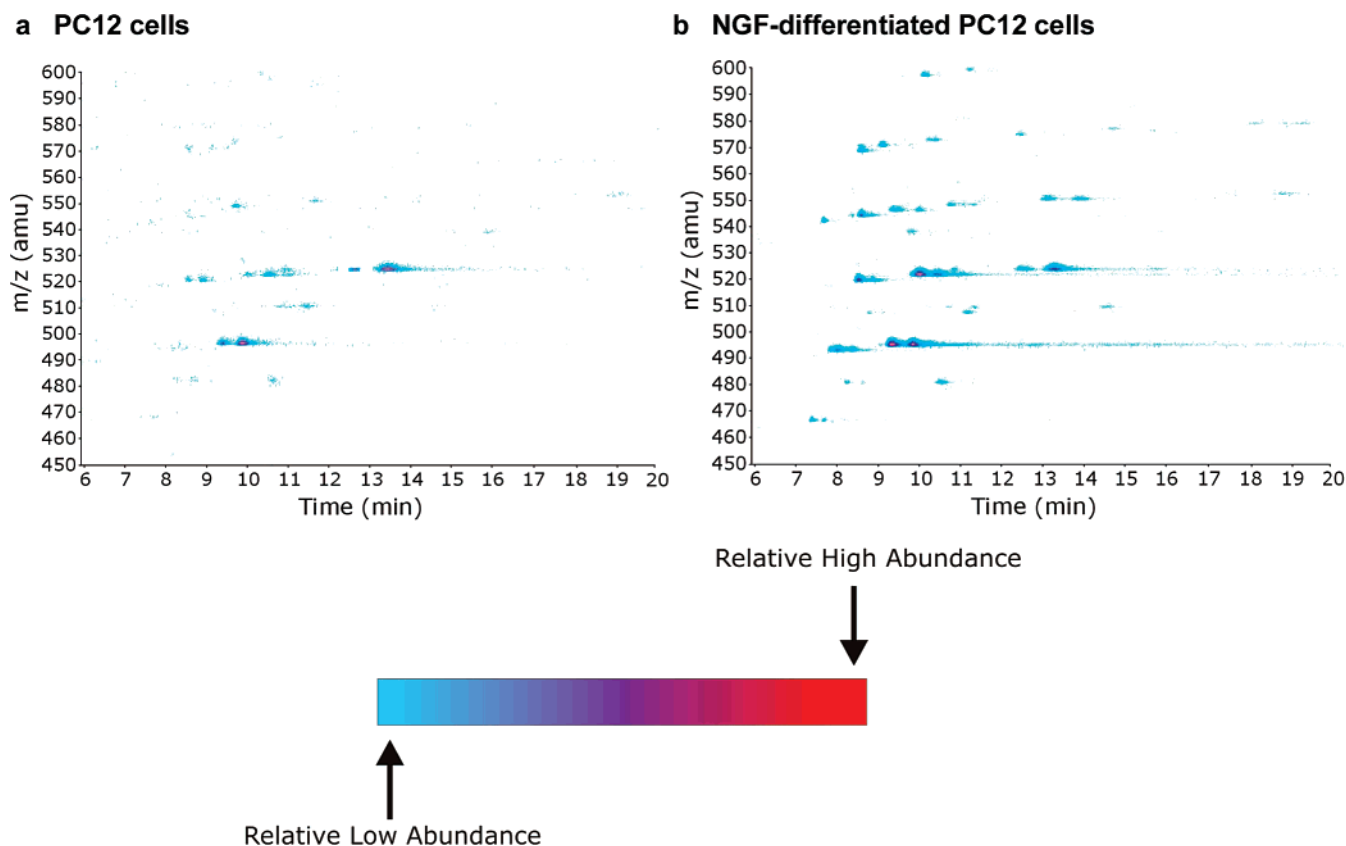


**Figure 2.** Glycerophosphocholine profiles of PC12 cells over the course of differentiation to a neuronal phenotype. 2D maps of mass versus elution time with relative lipid abundance from (a) PC12 cells and (b) PC12 cells differentiated to a neuronal phenotype. Spectra were obtained for glycerophospholipids and analyzed in positive ion mode using a precursor ion scan for an MS/MS fragment with a  $m/z$  of 184.0 to detect phosphocholine-containing subspecies. Spectra were extracted and plotted using Analyst 1.4.1 with color used to represent relative abundance. The experimental conditions of the LC–MS/MS are described in the text.

endogenous standard (C16:0 LPC with an  $m/z$  of 496.3 and elution time of 9.60 min). Normalization was performed to circumvent the fluctuation of the intensity of ion signals from run to run. This standardization protocol with endogenous C16:0 LPC gave identical results as normalization to the C13:0 LPC internal standard thereby enabling us to eliminate additional steps involved with spiking an exogenous lipid standard. Data on the regression curve are expressed as the mean of the triplicates  $\pm$  standard deviation. Concentrations of the native PAF species were calculated using the regression curve when  $y = 0$  and expressed as the mean of the triplicate samples  $\pm 95\%$  confidence interval. The 95% confidence interval was determined using Student's  $t$ -test. PAF species data were then standardized to total cell number and expressed as  $\text{pg}/10^6$  cells.

## RESULTS AND DISCUSSION

**Profiling Glycerophospholipid Changes by 2D Map.** Glycerophospholipid extracts from PC12 cells and PC12 cells differentiated to a neuronal phenotype for 7 days were obtained and analyzed in positive ion mode (Supporting Information (SI) Figure S-1). Typical spectra are presented as 2D maps of mass versus elution time with relative glycerophospholipid abundance indicated in color (SI Figure S-1). Changes in glycerophosphocholine subclasses were further assessed using a precursor ion scan for an MS/MS fragment with a  $m/z$  of 184.0 representing ionized phosphocholine, and candidate species were identified on the basis of theoretical mass (Table 1).

Three key characteristics are evident (Figure 2). First, the 2D maps were reproducible over multiple runs ( $n = 6$  per condition). As well, the maps of PC12 and differentiated PC12 could be readily manually aligned. Variation on the mass axis was on average 0.13 Da and 0.4 min on the elution time axis ( $n = 12$  spectra) and did not vary between conditions (precursor vs NGF-differentiated). Hence, specialized alignment software was not required to compare glycerophosphocholine profiles (Table 1). Second, a marked increase in the number of glycerophosphocholine species was detected in NGF-treated PC12 cells (Figure 2b) compared to undifferentiated precursors (Figure 2a) despite an overall decrease in glycerophospholipids observed following differentiation (SI Figure S-1). Third, the number of glycerophosphocholine species detected within the scan range of 450–600 Da is higher than the same  $m/z$  range previously observed for mouse B-cell NS-1 cells.<sup>33</sup> This is likely attributed to our utilization of nanoflow rate HPLC and a more sensitive mass spectrometer but may also reflect cell-specific differences in lipid metabolism.

**Normalization and Quantitation Based on Standard Addition.** Further mechanistic insight into the role of these changes in glycerophosphocholine families in developing neurons requires an efficient and sensitive means of identifying and quantifying individual molecular species. To this end, we focused on developing a quantitative analysis of changes in the phosphocholine-PAF species predicted to increase over the course of neuronal differentiation (Table 1) in the 2D screening spectra (Figure 2). We

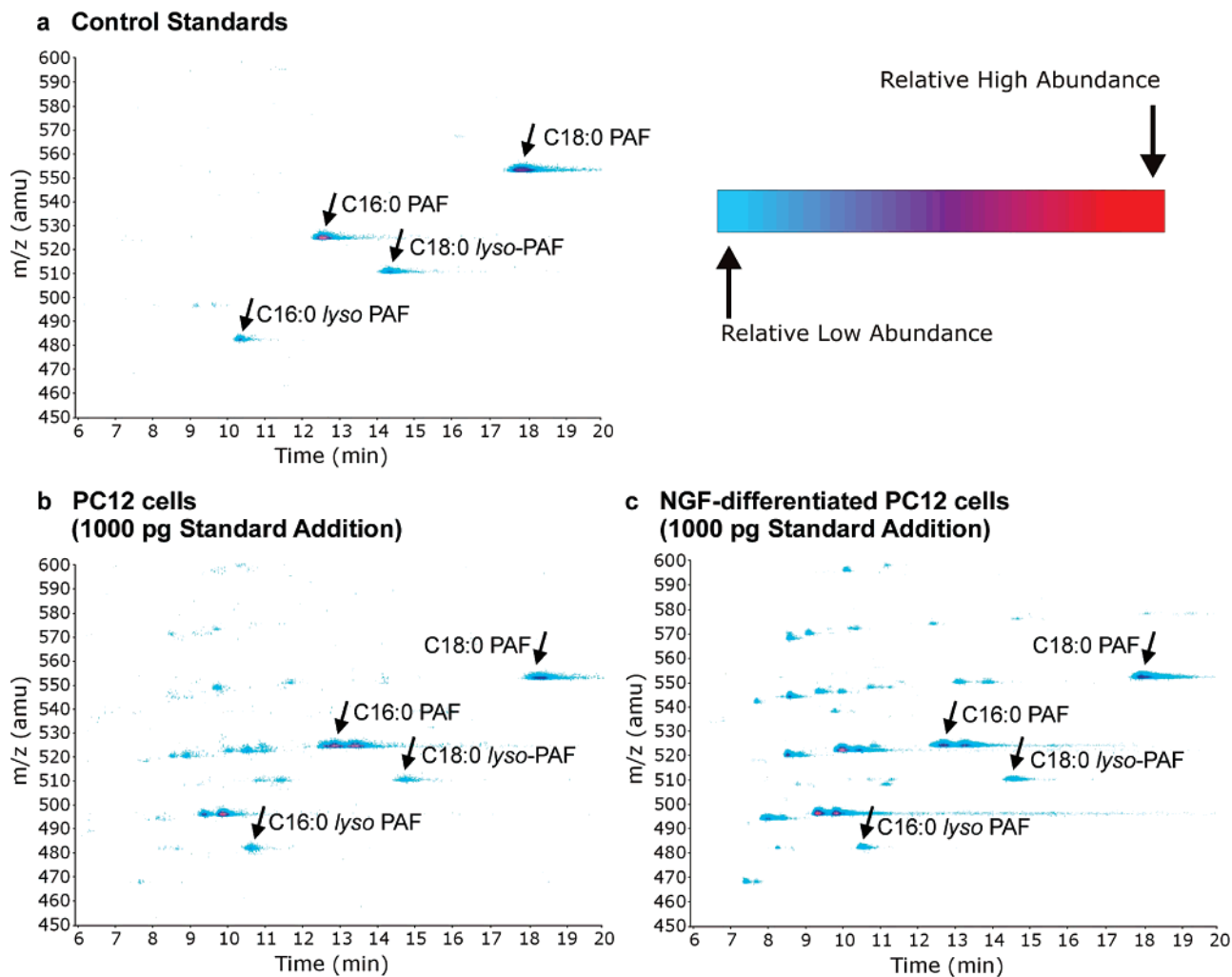


**Figure 3.** Identification of key PAF species from PC12 cells and PC12 cells differentiated to a neuronal phenotype. 2D spectra of mass versus elution time for (a) 1000 ng of C16:0, C18:0 PAF and C16:0, C18:0 *lyso*-PAF standards, (b) PC12 glycerophospholipid extracts spiked with 1000 ng of C16:0, C18:0 PAF and C16:0, C18:0 *lyso*-PAF, and (c) glycerophospholipids extracted from PC12 cells differentiated to a neuronal phenotype spiked with 1000 ng of C16:0, C18:0 PAF and C16:0, C18:0 *lyso*-PAF. The experimental conditions of the LC–MS/MS are described in the text.

selected three PAF species (C16:0 PAF, C16:0 *lyso*-PAF, C18:0 *lyso*-PAF) predicted to change over the course of neuronal differentiation in our 2D screen and one PAF species not detected in either PC12 or differentiated PC12 profiles (C18:0 PAF) for further analysis and absolute quantitation (Figure 2 and Table 1). To develop standard curves, four synthetic PAF standards with defined *sn*-1 and *sn*-2 chains and a phosphocholine *sn*-3 headgroup were used. These standards were C16:0, C18:0 PAF and C16:0, C18:0 *lyso*-PAF, where 16: represents the carbon atoms and :0 indicates the number of double bonds at the *sn*-1 position. We included C18:0 PAF as a negative control as our analysis predicted that the octadecyl-PAF species was present at concentrations below detectable levels in both PC12 and NGF-differentiated PC12 cells.

The absolute quantitation of these PAF species was performed through the standard addition method. Clear mass/elution time resolutions of combined standards were evident in 2D spectra (Figure 3a); however, these profiles provide qualitative not quantitative evidence of changes given that the dynamic range of the color coding of relative abundance generated by Analyst software is limited. Thus, the contrast required for detection of

lipids in lower abundance (i.e.,  $m/z$  510.5 C18:0 *lyso*-PAF eluting at 14.23 min) clearly saturates lipids at higher abundance (i.e.,  $m/z$  496.3 C16:0 LPC eluting at 9.60 min) (Figure 2). Moreover, the saturation of the images causes tailing of the peak to be overemphasised even with pure standards (Figure 3a). Fortunately, the dynamic range of the mass spectrometer is sufficient not to cause saturation of the signal in the MS traces and the XIC traces. Hence, as a screening tool, the 2D spectra provide a rapid means of identifying changing species that can then be validated by closer examination of XICs for each predicted species (Figure 4a–d) and quantitated by standard addition (Figure 5).

To validate our identification of our four test species and ensure that inclusion of molar excesses of standards would not mask detection of endogenous glycerophosphocholine species in our biological samples, we spiked lipid extracts from PC12 and NGF-differentiated PC12 cells with 0–1000 pg of the synthetic standards (Figure 3b,c). Spiked standards were clearly visible and did not impact upon detection of endogenous species when 2D spectra of “neat” (Figure 2a,b) and “spiked” samples (Figure 3b,c) were compared. Indicated species (C16:0, C18:0 PAF and C16:0, C18:0

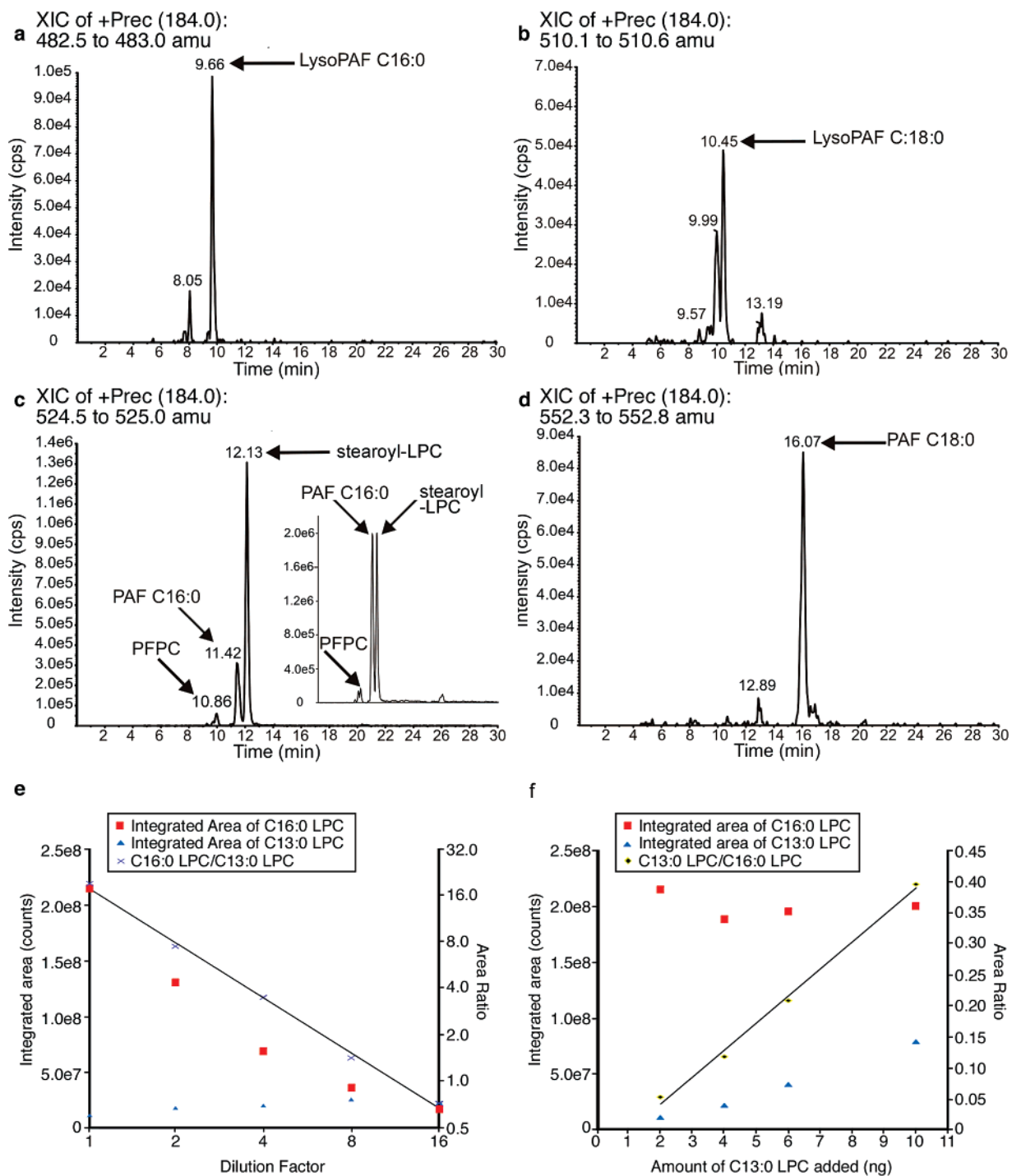


**Figure 4.** Identification and validation of PAF species quantitation using an internal standard (C13:0 LPC) and an endogenous standard (C16:0 LPC). (a–d) XICs are shown for PC12 cell lipid extracts spiked with 200 ng of each standard identifying (a) C16:0 *lyso*-PAF, (b) C18:0 *lyso*-PAF, (c) C16:0 PAF, and (d) C18:0 PAF. In (c), the peaks eluting at 10.86 and 12.13 min are consistent with previous reports of PFPC and stearyl-LPC separation, respectively,<sup>40</sup> a glycerophospholipid isobaric with C16:0 PAF. Inset depicts PC12 cell extracts spiked with 1000 pg of C16:0 PAF demonstrating the specific increased peak intensity. Peak retention times were calculated by the instrument software (Analyst 1.4.1) and were  $\pm 0.4$  min between MS runs. (e) To validate our use of C16:0 LPC as an endogenous standard, the same PC12 lipid extract was serially diluted and integrated peak intensity for C16:0 LPC ( $m/z$  496.3, elution time 9.60 min) standardized against an internal standard was plotted (red boxes and left axis). In each diluent, the internal standard was 2 ng of C13:0 LPC not naturally synthesized by mammalian cells (blue triangles and left axis). A significant linear relationship ( $R^2 = 0.997$ ) was observed between the area ratio of C16:0 LPC/C13:0 LPC and the dilution factor following normalization of C16:0 LPC to C13:0 LPC (blue Xs and right axis). (f) To further establish the linear range of response, 1–10 ng of the synthetic internal standard (C13:0 LPC) was added to the same experimental analyte containing the same theoretical amount of (C16:0 LPC). Variations in the integrated peak area of C16:0 LPC between quadruplicate MS runs are indicated by the red boxes (left axis) and the integrated peak of C13:0 LPC by the blue triangles (left axis). To correct peak intensity for variations across MS runs, the area ratio of C13:0 LPC/C16:0 LPC was calculated (black dots) and demonstrates a linear relationship with the amount of C13:0 LPC added (yellow triangles and right axis,  $R^2 = 0.995$ ).

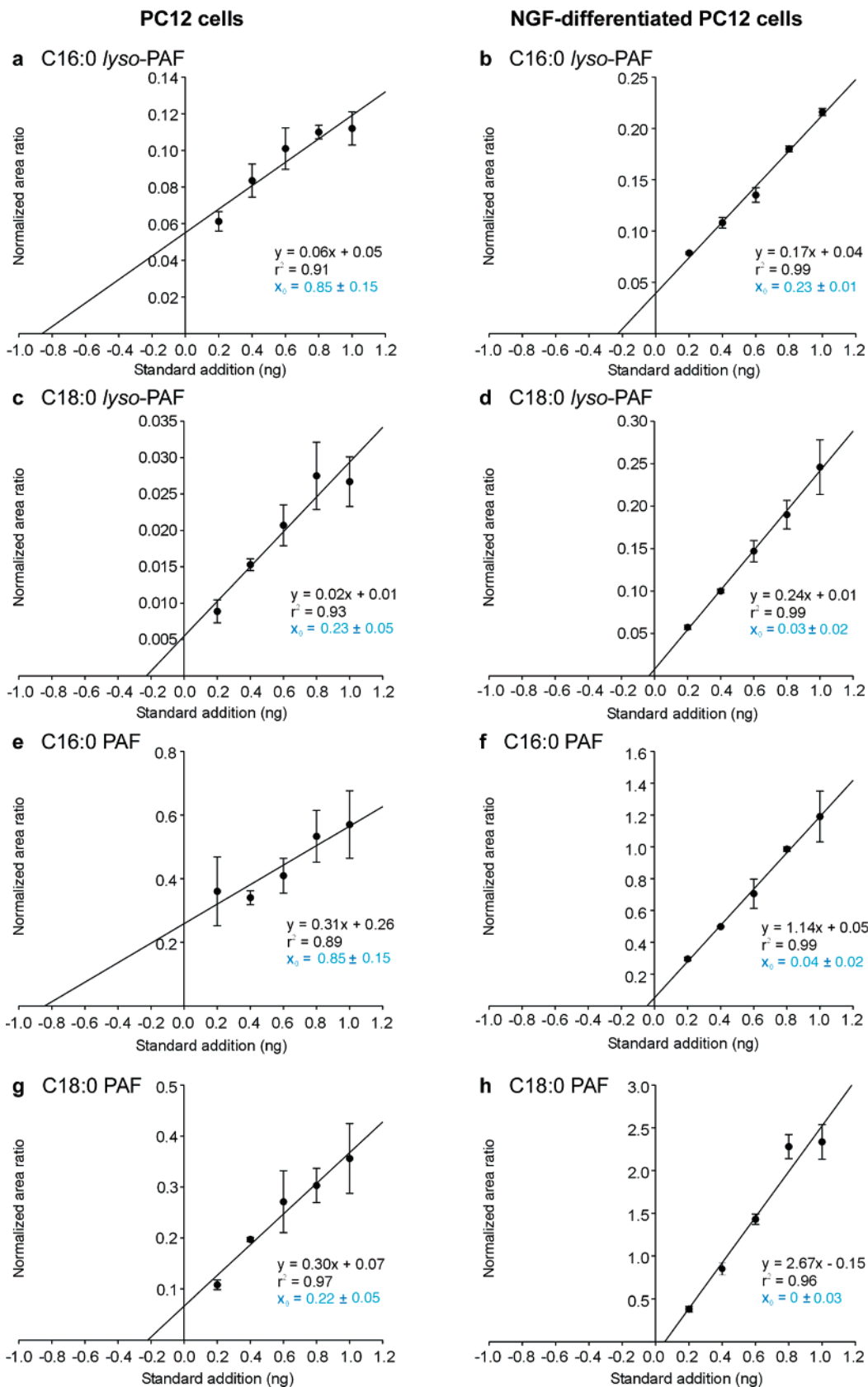


**Figure 5.** Quantitation of PAF species from PC12 cells and PC12 cells differentiated to a neuronal phenotype. Lipid extracts from PC12 cells (total cell number  $1.79 \times 10^7$ ) and PC12 cells differentiated to a neuronal phenotype (total cell number  $2.34 \times 10^6$ ) were spiked with 200, 400, 600, 800, or 1000 ng of C16:0, C18:0 PAF and C16:0, C18:0 lyso-PAF and analyzed in positive ion mode followed by a precursor ion scan for masses having an  $m/z$  184.0 MS/MS fragment. Each standard addition was repeated in triplicate. Corresponding peaks of interest were identified ( $m/z$  482.4, 524.3, 510.4, 552.4) and were normalized against the endogenous C16:0 LPC standard to account for any trial variability within each standard addition point. Native PAF species from the cell samples were calculated from the  $x$ -intercept using linear regression. Data points depict mean of triplicate measurements  $\pm$  standard deviation.

*lyso*-PAF) were confirmed using the standard addition method (Figures 3 and 4a–d). XICs are shown for the four species in Figure 4a–d, respectively. Major PAF species were identified by MS scan for their protonated molecule at expected  $m/z$  and by precursor ion scan for a phosphocholine product ion at  $m/z$  184 (Figures 2 and 3). Because the predicted ion transitions are not necessarily specific for PAF given multiple isobaric glycerophospholipids, identification was confirmed by closer examination of the chromatographic separations (Figure 3a–d). For example, 1-hexadecanoyl-2-formyl-glycerophosphocholine (PFPC), which is isobaric with C16:0 PAF,<sup>39</sup> elutes earlier than C16:0 PAF whereas stearyl-LPC elutes later (Figure 4d) as previously reported<sup>40</sup> and can be clearly separated and identified in the XICs (Figure 4c).

For quantitative analysis of PAF species, we compared two methods to standardize for variations between MS runs. First, equal amounts (2 ng) of a synthetic internal standard C13:0 LPC not naturally produced by mammalian cells<sup>38</sup> were added to serially diluted PC12 lipid analytes. The integrated peak intensities of endogenous C16:0 LPC ( $m/z$  496.3, elution time 9.6 min) in each sample were standardized to that of the spiked internal standard C13:0 LPC (Figure 4e). A linear response was established with normalized peak intensities corresponding to C16:0 LPC falling within linear range between analyte dilution factors of 1–16. The second experiment (Figure 4f) reverses the conditions. We maintained the same sample concentration but added increasing amounts of C13:0 LPC. The expected linear response was observed when integrated peak intensities of C13:0 LPC were normalized to the endogenous standard C16:0 LPC (Figure 4f) thereby validating our use of this endogenous lipid standard to control for variations between MS runs.

We have also evaluated the analytical limit of detection of our approach for two species that are not endogenously present in the sample (C13:0 LPC and C18:0 PAF) added to a lipid extract from differentiated cells. The limit of detection, defined as the chromatographic peak height divided by three times the standard deviation in the baseline, was measured to be  $1.7 \pm 0.7$  pg for C13:0 LPC and  $2.0 \pm 0.7$  pg for C18:0 PAF. We have also evaluated the accuracy of absolute quantitation by the standard addition method using spike samples of 200 pg of C16:0 PAF and C18:0 *lyso*-PAF in differentiated PC12 cell lipid extracts as reference standards. These reference standards were then quantified by the standard addition method and we respectively measured levels of  $200 \pm 25$  and  $200 \pm 22$  pg. These results indicate that we are accurate within ~10% of the value 95% of the time. The analytical limit of detection and the assessment of the accuracy clearly demonstrate that the analytical technique is suitable to measure a very low level of glycerophospholipids.

The standard addition method was used to quantify the absolute levels of the PAF subspecies present in the sample (Figure 5). Each standard addition containing 200, 400, 600, 800, and 1000 pg of C16:0, C18:0 PAF and C16:0, C18:0 *lyso*-PAF was repeated in triplicate. Peaks of interest were identified ( $m/z$  482.4, 524.3, 510.4, 552.4), and their areas were calculated using Analyst software. The endogenous PAF species C16:0 LPC ( $m/z$  496.3,

**Table 2. LC–MS/MS Quantitation of PAF in PC12 Cells and NGF-Differentiated PC12 Cells.**

PAF species	WT-PC12 (ng/10 <sup>6</sup> cells)	NGF- differentiated PC12 (ng/10 <sup>6</sup> cells)
C16:0 <i>lyso</i> -PAF	1.79 ± 0.31	29.01 ± 1.77
C18:0 <i>lyso</i> -PAF	0.48 ± 0.10	4.27 ± 1.01
C16:0 PAF	1.77 ± 0.31	5.65 ± 1.01
C18:0 PAF	0.47 ± 0.46	0 ± 3.53

elution time 9.60 min) was used to correct the variation in intensity between the triplicate MS runs. This allowed for the correction in intensity variation within a standard addition experiments related to one sample due to changes in alignment and MS performances. Native PAF subspecies concentrations were then determined from the  $x$ -intercept using linear regression analysis (Figure 5a–f). Cook's distance analysis of residuals was performed to identify sample outliers that aberrantly influenced regression outcome.<sup>41</sup> The absolute levels of PAF species were corrected according to the number of cells utilized. Data were expressed as ng/10<sup>6</sup> cells (Table 2). Comparison of these results with our analysis of the limit of detection indicates that the bulk of the contribution to the error comes from the biological variability of the two states of PC12 cells between cultures. Results clearly indicate a 16-fold increase in C16:0 *lyso*-PAF, an 8-fold increase in C16:0 PAF, and a 3-fold increase in C18:0 *lyso*-PAF. C18:0 PAF levels remained below level of quantitation by the standard addition method and were not identified in either PC12 cells or NGF-differentiated PC12 cells.

## CONCLUSIONS

Here, we describe a rapid means of profiling changes in glycerophospholipids with identification and quantitation of glycerophosphocholine species following induction of neuronal differentiation. The combination of nanoflow rate HPLC with ESI-MS in different modes facilitated comparison of multiple species in total lipid 2D maps. In this study, we show that the standard addition of synthetic PAF subspecies allows for the absolute quantitation of the changes in PAF family members following neuronal differentiation. Surprisingly, a marked asymmetry was detected in the two predominant PAF species (C16:0, C18:0) produced by NGF-treated PC12 cells. Differentiation to a peripheral neuronal phenotype was associated with increases in C16:0 PAF and, more dramatically, with production of its immediate precursor and metabolite C16:0 *lyso*-PAF. C18:0 PAF was below the limits of detection in both PC12 precursors and differentiated neurons. Interestingly, C18:0 *lyso*-PAF levels were elevated, albeit at much lower concentrations than C16:0 *lyso*-PAF. When placed in context with evidence that C18:0 PAF increases in neural fluids following neuropathological challenge,<sup>25</sup> these data suggest a difference between PAF molecular species produced by differentiating and damaged neurons quantifiable by this analytical technique. The methodology described here will enable a means of screening and comparing changes in glycerophospholipids, specifically PAF species, by neurons and glia during central and peripheral nervous system development and over the course of progressive neurodegenerative disease. This quantitation is critical

(39) Harrison, K. A.; Clay, K. L.; Murphy, R. C. *J. Mass Spectrom.* **1999**, *34*, 330–335.

(40) Owen, J. S.; Wykle, R. L.; Samuel, M. P.; Thomas, M. J. *J. Lipid Res.* **2005**, *46*, 373–382.

(41) Demidenko, E.; Stukel, T. A. *Stat. Med.* **2005**, *24*, 893–909.

to pursuing mechanistic insight in the role of glycerophospholipids in neuronal differentiation and death.

#### **ACKNOWLEDGMENT**

This research was supported by an Ontario Mental Health Foundation (OMHF) operating grant to S.A.L.B. and D.F. S.A.L.B. is a Canadian Institute of Health Research New Investigator and an OMHF Intermediate Investigator. D.F. is a Canadian Research Chair. R.D. is a recipient of a Natural Sciences and Engineering Undergraduate Research Studentship Award. A.B. was a recipient of an Ontario Genomics Institute Summer Fellowship award. We

thank Jim Bennett for editorial assistance. S.N.M., W. H., and M.E. contributed equally.

#### **SUPPORTING INFORMATION AVAILABLE**

Additional information as noted in text. This material is available free of charge via the Internet at <http://pubs.acs.org>.

Received for review June 11, 2007. Accepted September 12, 2007.

AC0712291